Study on the Effect of Long Shroud Structure on Molten Steel Flow in Single Strand Tundish by Numerical Simulation

Ai-ping Zhang, Ming-mei Zhu, and Jie Luo

Abstract In this paper, a single strand tundish is taken as the research object, and a three-dimensional mathematical model is established to analyze the effect of the long shroud structure on the flow field, temperature field, pressure field, and inclusions trajectories of molten steel in the tundish. The fluid flow patterns in the tundish are analyzed by comparing the residence time distribution curves of the four types of long shrouds: traditional long shroud vortex long shroud, dissipative long shroud, and trumpet-shaped long shroud. At the same time, the effects of different long shroud structures on the fluctuation of free surface are compared. The reasonable long shroud structure is conducive to obtaining uniform molten steel and provides theoretical guidance for actual production.

Keywords Long shroud · Tundish · Residence time distribution curve · Numerical simulation · Fluctuation of free surface

Introduction

The molten steel injected into the tundish from the ladle through the shroud has great impingement on the steel in the tundish impact zone. When the fluctuation of the liquid level is too large, the molten steel will be involved in slag inclusion and secondary oxidation, which will reduce the purity of the molten steel and affect the internal quality of the cast slab.

Morales-Higa and Solorio-Diaz et al. [1, 2] proposed a dissipative shroud. Compared with the traditional long shroud and vortex shroud, the dissipative shroud can reduce the turbulent kinetic energy of the molten steel flowing to the tundish, therefore, it allows for obtaining a more stable slag layer and facilitating the contact between the inclusions and the free surface. Rodolfo and Garcia-Hernandez et al. [3, 4] used numerical simulation and water simulation methods to study the slag

A. Zhang · M. Zhu (✉) · J. Luo
College of Materials Science and Engineering, Chongqing University, Chongqing 400044, China
e-mail: zhumingmei@cqu.edu.cn

J. Lee et al. (eds.), *Materials Processing Fundamentals 2021*, The Minerals, Metals & Materials Series, https://doi.org/10.1007/978-3-030-65253-1_3

entrainment and gas entrainment phenomenon of traditional long shroud and dissipative shroud during package change (i.e. the process of molten steel from ladle to tundish). The large turbulent kinetic energy of the fluid flowing out of the traditional long shroud causes unstable three-phase flow, which is more likely to cause slag entrainment; however, the turbulent energy dissipation of the fluid flowing out of the dissipative shroud increases and the velocity of flowing into the tundish decreases. Solorio-Diaz et al. [5] used numerical simulation to calculate the fluid flow conditions and inclusion removal rates of the vortex shroud and different flow control devices at two different mass flow rates. The results show that the use of vortex shroud can replace the role of flow control device. Zhang et al. [6] used large eddy simulation to study the fluid flow process in the traditional long shroud and trumpet shroud, the fluid flowing through the trumpet area can be mixed with the surrounding fluid well, dissipating turbulent kinetic energy and reducing the velocity of the fluid flowing into the tundish. Zhang et al. [7] added two trumpet long shroud on the basis of the traditional long shroud. Three types of shrouds are used in combination with two different turbulence suppressors to study the steady-state and three-dimensional multiphase flow during package change. The results show that the trumpet shroud can reduce the turbulent kinetic energy of the fluid flowing into the tundish; as the inner diameter of the trumpet shroud increases, the area formed by the free surface slag hole decreases.

In summary, obtaining an ideal flow pattern and clean molten steel, and reducing the excessive impact of molten steel in the injection zone of the tundish, can be achieved by designing different shroud structures. This paper mainly investigates the influence of four different shroud structures, including traditional long shroud, vortex shroud, dissipative shroud and trumpet shroud, on the flow field, temperature field and pressure field of molten steel in the tundish. The residence time distribution (RTD) curve is used to analyze the fluid flow pattern in the tundish under different shroud structures and to compare the liquid level fluctuations under four different shroud structures.

Model Hypothesis

In order to facilitate the study of the flow phenomenon in the tundish, this study has the following assumptions: the flow of molten steel in the tundish is a steady-state incompressible viscous fluid; the inclusions are spherical particles and the movements are independent of each other; the effect of temperature on flow is negligible; density and viscosity are constant; the flow of molten steel is turbulent.

Model Formulation

The flow of molten steel in the continuous casting tundish is a three-dimensional turbulent flow, and the mass equation, momentum equation, energy equation and turbulent kinetic energy equation used in the calculation are as follows [8].

Continuity equation:

$$\frac{\partial P}{\partial t} + \frac{\partial(\rho\mu_i)}{\partial x_i} = 0 \tag{1}$$

Momentum equation:

$$\frac{\partial\left(\rho\mu_i\mu_j\right)}{\partial x_j} = -\frac{\partial P}{\partial x_j} + \frac{\partial}{\partial x_j}\left(\mu_{\text{eff}}\frac{\partial\mu_i}{\partial x_j}\right) + \frac{\partial}{\partial x_i}\left(\mu_{\text{eff}}\frac{\partial\mu_j}{\partial x_i}\right) + \rho g_i \tag{2}$$

The model assumes that the flow field is turbulent, so standard k–ε equation is used to describe the turbulent viscosity coefficient:

$$\frac{\partial(\rho\mu_i)}{\partial x_i} = \frac{\partial}{\partial x_i}\left[\left(\mu_{\text{eff}} + \frac{\mu_t}{\sigma_k}\right)\frac{\partial k}{\partial x_i}\right] + G - \rho\varepsilon \tag{3}$$

$$\frac{\partial(\rho\mu_i\varepsilon)}{\partial x_i} = \frac{\partial}{\partial x_i}\left[\left(\mu_{\text{eff}} + \frac{\mu_t}{\sigma_\varepsilon}\right)\frac{\partial\varepsilon}{\partial x_i}\right] + c_1\frac{\varepsilon}{k}G - c_2\frac{\varepsilon^2}{k}\rho \tag{4}$$

among them

$$G = \mu_t\frac{\partial\mu_j}{\partial x_i}\left(\frac{\partial\mu_j}{\partial x_j} + \frac{\partial\mu_j}{\partial x_j}\right) \tag{5}$$

$$\mu_{\text{eff}} = \mu + \mu_t = \mu + c_\mu\rho\frac{k^2}{\varepsilon} \tag{6}$$

Energy equation related to temperature field calculation:

$$\rho\left(\frac{\partial T}{\partial t} + C_p\frac{\partial T}{\partial x_i}\right) = \frac{\partial}{\partial x_i}\left(k_{\text{eff}}\frac{\partial T}{\partial x_i}\right) \tag{7}$$

Equation of transport behavior of inclusions in tundish:

$$\frac{\mathrm{d}u_{\text{pi}}}{\mathrm{d}t} = \frac{18u}{\rho_{\text{p}}d_{\text{p}}^2}\cdot\frac{C_{\text{D}}\text{Re}}{24}\left(u_i - u_{\text{pi}}\right) + \frac{\left(\rho_{\text{p}} - \rho\right)}{\rho_{\text{p}}}g_{\text{p}} + F_i \tag{8}$$

Mass transfer equation of tracer in tundish:

$$\left(\frac{\partial C}{\partial t} + \nabla \times U_{\mathrm{c}}\right) = \nabla \times \left(\rho D_{\mathrm{c}} + \frac{\mu_{\mathrm{t}}}{\mathrm{Sc}_{\mathrm{t}}}\right)\nabla \times \left(\frac{C}{\rho}\right) + S_{\mathrm{C}} \tag{9}$$

The free liquid surface fluctuation range can be calculated by the following formula:

$$H = \frac{P_{\mathrm{sta}} - \overline{P_{\mathrm{sta}}}}{\rho |g|} \tag{10}$$

where ρ is the density, kg m^{-3}; u_i and u_j are the velocity of molten steel in the i and j directions, m s^{-1}; p is the pressure, Pa; μ_{eff} is the effective viscosity, kg m^{-1} S^{-1}; C_1, C_2, C_μ, C_k, C_ε are empirical constants, and their values are 1.44, 1.93, 0.99, 1.0, 1.3; k_{eff} is the effective thermal conductivity, W m^{-1} K^{-1}; ρ_{p} is the particle density, kg m^{-3}; d_{p} is the particle diameter, m; u_{pi} is the particle velocity, m s^{-1}; C_{D} is the drag coefficient; Re is the relative Reynolds coefficient; F_i is the force, N; S_{c} is the volume source phase, is the residual mass per unit volume of the tracer unit time, kg/(m^3 s); D_{c} tracer diffusion coefficient, this paper takes 1.1×10^{-8} m^2/s; μ_{t} is the turbulent viscosity of molten steel, kg/(m s); SC_{t} is the turbulent Schmidt number of the tracer, taken 0.9. H represents the z-axis coordinate value of the free surface of the molten pool in the coordinate system of (x, y, z), which is consistent with the direction of gravity, P_{sta} is the static pressure value of the unit calculated by the free surface, and $\overline{P_{\mathrm{sta}}}$ is the average static pressure value of the free surface [9].

Boundary Conditions

In this paper, the ladle nozzle is the velocity inlet, the outlet is defined as the pressure outlet, the liquid–solid interface is the non-slip boundary, and the velocity value on the solid wall is 0. The free surface is the zero shear stress surface, and the heat radiation loss of the wall and the free surface is negligible (the schematic diagram is shown in Fig. 1). Inclusion particles are removed by the adsorption of the slag layer on the surface of the molten steel, and the inclusions that touch the wall of the tundish are regarded as rebound.

Calculation Method

The ratio of the tundish model to the actual object is 1:1, and the model grid is divided into uniform unstructured grids (see Fig. 1 for details).

The standard k–ε equation is used to describe the turbulence process, the energy equation is used to calculate the temperature field, the pressure coupling equations are used to solve the semi-implicit method (SIMPLE method), and the convergence residual value is less than 10^{-5}.

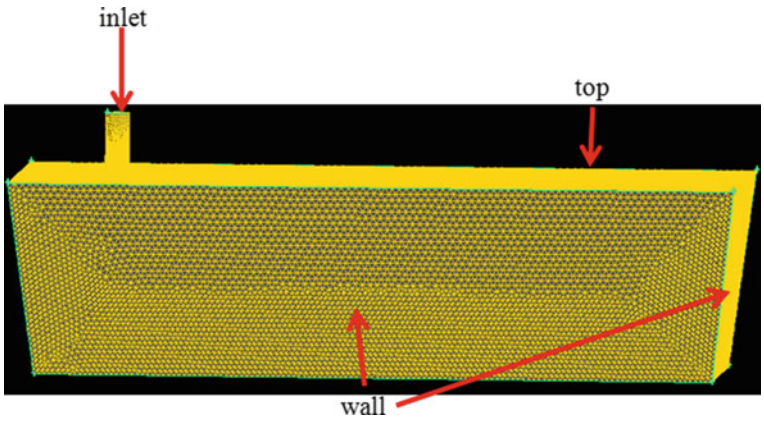

Fig. 1 Tundish meshing diagram. (Color figure online)

Table 1 Important physical parameters for simulation of fluid flow in tundish [10, 11]

Parameters	Values	Parameters	Values
Viscosity	0.0067 kg m^{-1} s^{-1}	Thermal conductivity	41 W m^{-2} K^{-1}
Specific heat	750 J kg^{-1} K^{-1}	Free surface heat flow	15 kW m^{-2}
Density	7020 kg m^{-3}	Bottom wall heat loss	1.4 kW m^{-2}
Turbulent kinetic energy at the inlet	$0.01V_{in}{}^2$ m^2/s^2	Long wall heat loss	3.8 kW m^{-2}
Dissipation rate at the inlet	$K_{in}{}^{1.5}/R_{inlet}$ m^2/s^3	Short wall heat loss	3.2 kW m^{-2}
Inlet temperature	1823.00 K	Tracer diffusion coefficient	1.1×10^{-8} m^2/s

Regarding the inclusion particles as a discrete phase, the Lagrange particle tracking model and the discrete phase model (DPM) are used to calculate the removal rate of the inclusions in the tundish. The parameters that may be used in the numerical simulation of the tundish are shown in Table 1.

When analyzing the characteristics of the molten pool flow field, the k–ε two-equation model for calculating the flow field and the volume of fluid (VOF) two-phase flow model are coupled to calculate the characteristics of the molten pool liquid level fluctuation.

Simulation Scheme

Figure 2 is a schematic diagram of the continuous casting process. The four different shroud structures are traditional long shroud, vortex shroud, dissipative shroud and trumpet shroud. A simple diagram is shown in Fig. 3.

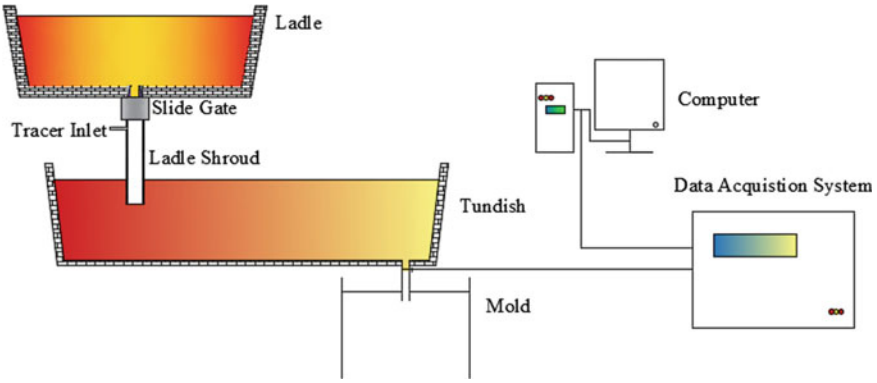

Fig. 2 Simplified diagram of the tundish continuous casting process. (Color figure online)

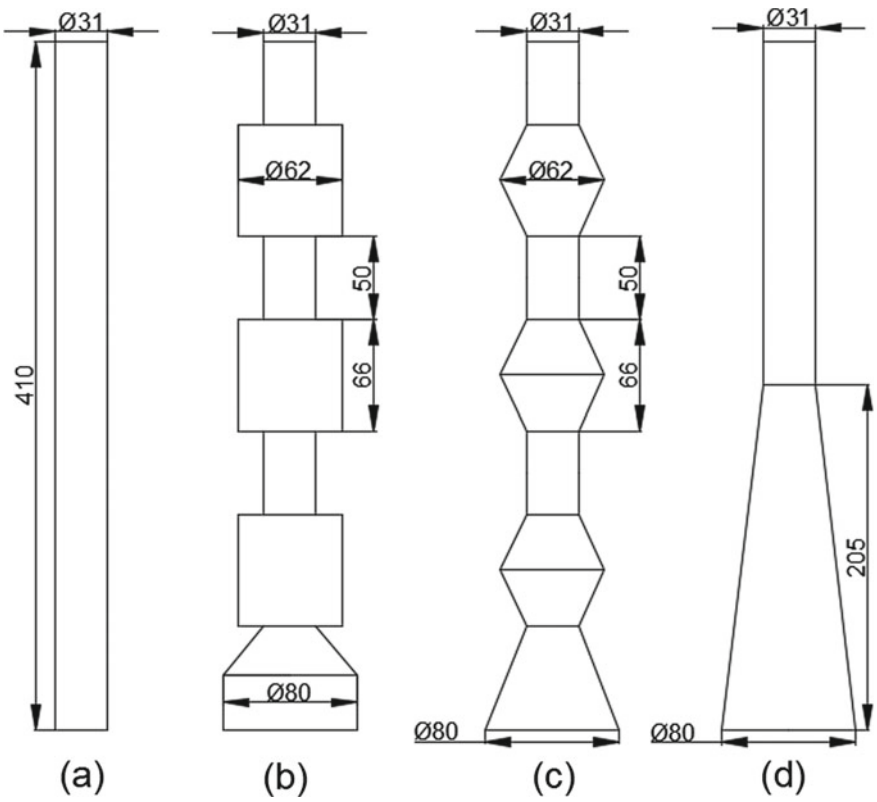

Fig. 3 Schematic diagram of different shrouds structure **a** traditional shroud; **b** vortex shroud; **c** dissipative shroud; **d** trumpet shroud

Results and Analysis

According to the above four different shroud structures, modeling in Gambit software, importing FLUENT calculation, finally after post-processing, the following results are obtained.

Flow Field Comparison

Figure 4 is the velocity cloud diagram of the center surface of the tundish exit and entrance of different shroud structures. It can be seen that the molten steel is injected into the tundish under the action of gravity and directly impacts the bottom of the tundish, and then a part of the molten steel flows upward to form a backflow. However, the impact strength of different shroud structures is different. By comparing the pressure value at the bottom of the tundish, it is found that the maximum impact pressure of the traditional long shroud is about 40,000 Pa, and the rest is about 27,000 Pa. At the same time, the reflux area (the extent of the green area in the picture) formed by the molten steel through the traditional long shroud is wider. The reason may be that the shroud of the other three structures has expansion or contraction parts, so a part of the turbulent strength of the molten steel is dissipated.

Temperature Difference

Figure 5 shows the average temperature of top and outlet. Although the former shows an upward trend, but in general, the maximum temperature difference is only 1.35 K. Considering the randomness of temperature distribution, the effect of four shrouds on the temperature of top and outlet cannot be identified.

RTD Curve and Flow Pattern

The concentration of the tracer in the tundish was calculated by the component transmission equation, and the RTD curve(i.e. dimensionless distribution function) was obtained after post-processing. It can be seen from Fig. 6 that the RTD curve of the traditional long shroud has a sharp peak, and the remaining peaks are relatively smooth. The reason may be that the strong turbulence is buffered when the molten steel passes through the abrupt shroud diameter of the latter, and the peak in the former may be caused by the instantaneous molten steel impact. However, the response time and the time to reach the peak concentration of the four different shroud structures

(a) Traditional shroud

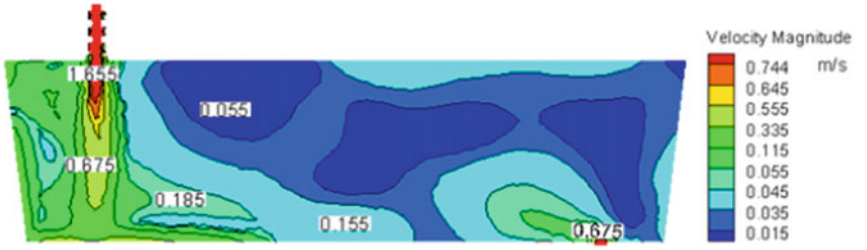

(b) Vortex shroud

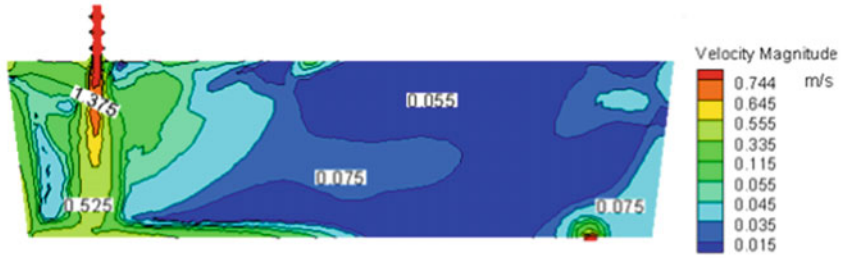

(c) Dissipative shroud

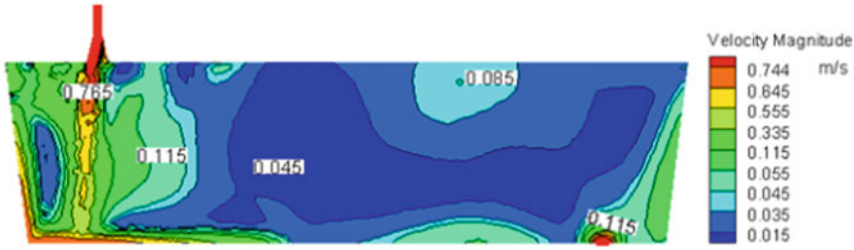

(d) Trumpet shroud;

Fig. 4 Speed cloud diagram of the center surface of the entrance and exit of the tundish. (Color figure online)

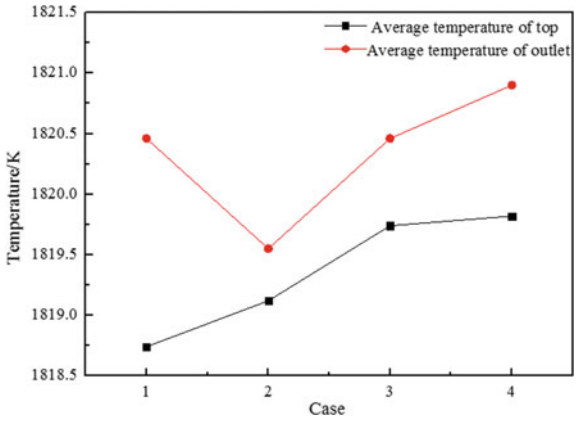

Fig. 5 Temperature difference in the tundish of different structures of the nozzle. (Color figure online)

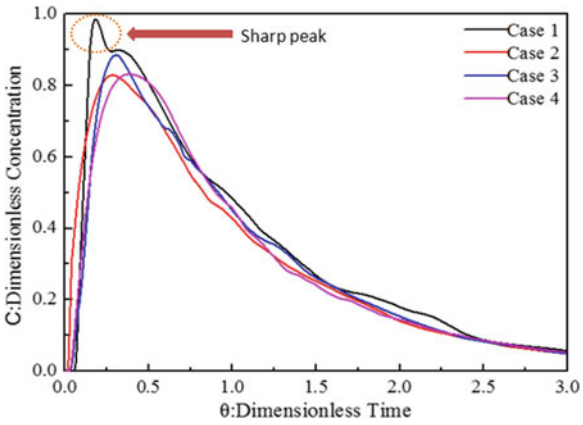

Fig. 6 RTD curve. (Color figure online)

are different. It can be inferred that the shroud structure has little effect on the flow pattern, mainly affecting the turbulence intensity of the inflowing molten steel.

Inclusion Removal Rate

Figure 7 shows the removal rate of inclusions(the amount captured by the top surface accounts for the total injected) in the tundish of the shroud with four different structures. It can be seen that the difference between the first two is small, but the removal rate corresponding to the dissipative shroud is slightly higher. The reason may be that the lower part of the shroud of Case 1 and Case 2 is a straight-through type, while Case 3 and 4 are a trumpet type, and the sudden change area of the trumpet type of Case 3 is greater than that of Case 4.

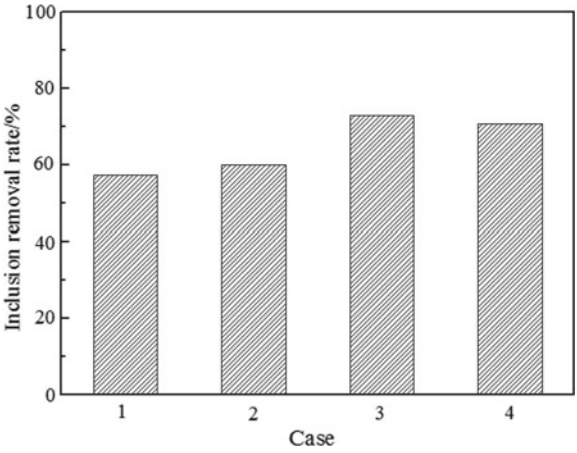

Fig. 7 Inclusion removal rate of different shroud structures

Liquid Level Fluctuation

Combining the k–ε two-equation model and the VOF model, the fluctuation of the tundish level during transient pouring is calculated. Figure 8 shows the center position of the short wall at a distance of 0 mm. It can be seen that the four cases are consistent: the fluctuation in the 350 mm area along the short wall is within 1 mm, while the fluctuation on both sides of the short wall is about 1.5 mm. Some even exceed 2 mm. Comparing the four cases, it can be seen that the traditional long shroud and the vortex shroud have significantly higher liquid level fluctuations than the dissipative shroud and the trumpet shroud; and the fluctuations of the first two are opposite, while the latter two have similar fluctuations. But a more accurate conclusion should be combined with water model experiments to illustrate. Different shroud structures

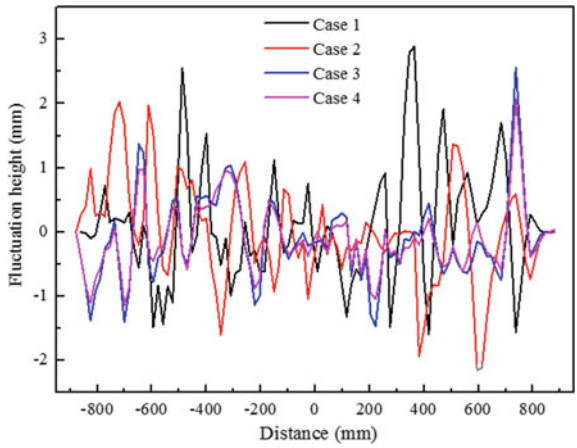

Fig. 8 Tundish liquid level fluctuations with different shroud structures. (Color figure online)

make the speed of the molten steel reach the impact zone different. The upward reflux increases the liquid steel exchange rate. When the molten steel flows along the bottom of the tundish to the outlet, the impact with the wall causes greater side fluctuations.

Conclusion

This paper compares four different shroud structures of traditional long shroud, vortex shroud, dissipative shroud, and trumpet shroud to analyze the flow in the tundish and the fluctuation of the liquid level. The turbulence intensity and pressure of molten steel passing through the traditional long shroud to the impact area are significantly higher than the other three types; however, the average temperature and inclusion removal rate of the four different shroud structures are similar, the liquid level on both sides of the short wall fluctuates larger than the central area, the liquid level fluctuations of the traditional long shroud and vortex shroud are opposite, and the liquid level fluctuations of the dissipative shroud and trumpet shroud are similar.

References

1. Morales-Higa K, Guthrie RIL, Isac M et al (2013) Ladle shroud as a flow control device for tundish operations. Metall Mater Trans B
2. Solorio-Diaz G, Davila-Morales R, Jose BS et al (2014) Numerical modelling of dissipation phenomena in a new ladle shroud for fluidynamic control and its effect on inclusions removal in a slab tundish. Steel Res Int 85(5):863–874
3. Morales RD, Calderon-Ramos I et al (2016) Multiphase flow modeling of slag entrainment during ladle change-over operation. Metall Mater Trans B
4. Garcia-Hernandez S, Morales RD, de Jesus Barreto J et al (2015) Modeling study of slag emulsification during ladle change-over using a dissipative ladle shroud. Steel Res Int
5. Solorio-Diaz G, Ramos-Banderas A, Barreto JDJ et al (2010) Modeling study of turbulent flow effect on inclusion removal in a tundish with swirling ladle shroud. Steel Res Int 80(3):223–234
6. Zhang J et al (2016) Comparative study of fluid flow and mass transfer in a trumpet-shaped ladle shroud using large eddy simulation. Metall Mater Trans B 47(1):495–507
7. Zhang H, Fang Q, Deng S et al (2019) Multiphase flow in a five-strand tundish using trumpet ladle shroud during steady-state casting and ladle change-over. Steel Res Int 90(3)
8. Zhang J, Yang S, Li J et al (2015) Large eddy simulation on flow structure in a dissipative ladle shroud and a tundish. ISIJ Int 55(8):1684–1692
9. Morales-Higa K, Guthrie RIL, Isac M et al (2013) Ladle shroud as a flow control device for tundish operations. Metall Mater Trans B 44(1):63–79
10. Chatterjee S, Li D, Chattopadhyay K (2018) Modeling of liquid steel/slag/argon gas multiphase flow during tundish open eye formation in a two-strand tundish. Metall Mater Trans B 49(2):756
11. Qin X-F, Cheng C-G, Li Y et al (2019) A Simulation study on the flow behavior of liquid steel in tundish with annular argon blowing in the upper nozzle. Metals 9(2):225